Nuclear Physics B140 (1978) 449–467
© North-Holland Publishing Company

GLUONS IN QUARKONIUM DECAY

K. KOLLER
Sektion Physik, Universität München, Germany

T. WALSH
Deutsches Elektronen-Synchroton DESY, Hamburg, Germany

Received 7 April 1978

We discuss what can be learned from the $^3S_1$ quarkonium decay

$Q\bar{Q} \to 3$ gluons ,

$Q\bar{Q} \to \gamma + 2$ gluons .

The former is a way to find gluon jets and test QCD. The latter also allows us to measure

gluon + gluon $\to$ hadrons ,

and look for pure gluonic resonances (glueballs).

1. Introduction

Quantum chromodynamics (QCD) is the non-Abelian gauge theory of quarks with flavor and color interacting with massless colored vector gluons [1]. Convincing evidence for confined colored quarks comes from the spectroscopy of $q\bar{q}$ and qqq hadrons and from lepton-hadron processes, particularly from quark jets in $e^+e^- \to q\bar{q} \to 2$ jets [2]. Similarly convincing evidence for gluons is lacking. The existence of gluon jets [3] (in analogy to quark jets), and also of hadrons made solely out of gluons [4] (called glueballs) would be objective evidence for QCD's gluons. Since the theory has quarks and gluons confined inside hadrons and not free, this is probably the best and most direct evidence we can expect to find.

With the aim of finding gluons and checking the predictions of QCD, we examine the processes [5]

$$e^+e^- \to Q\bar{Q} \to \begin{cases} 3 \text{ gluons} \to 3 \text{ jets} , \\ \\ \text{photon} + 2 \text{ gluons} \to \gamma + \text{hadrons} , \end{cases} \qquad (1)$$

where $Q\bar{Q}$ stands for a heavy narrow ground state $^3S_1$ "quarkonium" state (e.g. Υ (9.4), which we assume is $Q\bar{Q}$).

$Q\bar{Q} \to 3g$ is the direct decay mechanism of ortho-quarkonium in QCD [6] ($Q\bar{Q} \to 1\gamma \to q\bar{q}$ is also present, of course); $Q\bar{Q} \to \gamma + 2g$ is particularly useful [7] as the rate *and* the energy and angular distribution of the photon are predicted by the theory.

If the directly produced photon in $Q\bar{Q} \to \gamma + 2g$ can be identified on an event-by-event basis, this reaction offers a way to study gluon jets complementary to $Q\bar{Q} \to 3g$. More importantly, it offers a way to *measure* the process

$$g + g \to \text{hadrons} \tag{2}$$

for gluon-gluon invariant masses from zero to $M_{Q\bar{Q}}$. At low invariant masses *

$$Q\bar{Q} \to \gamma + 2g \to \gamma + (C = + \text{ glueball}) \tag{3}$$

may lead to the discovery of such states. If we apply the Zweig [8] rule to gluons just as to quarks, (3) is even the favored way to look for glueballs.

Most current evidence for QCD comes from comparison of predicted QCD radiative corrections and deep inelastic experiments [9] **. Process (1) tests the theory to lowest non-vanishing order in the Q^2 dependent QCD coupling $g_S = (4\pi\alpha_S(Q^2))^{1/2}$ (the Born approximation). For this reason we consider it to be especially important.

In sect. 2 we work out gluon and photon distributions in (1). The γ distribution in $Q\bar{Q} \to \gamma + 2g$ can be directly compared to experiment. This is harder for $Q\bar{Q} \to 3g$. However, we point out that for sufficiently large $M_{Q\bar{Q}}$ the total gluon jet three-momentum can be measured in principle, e.g. by calorimetry. This depends only on the assumption of bounded p_T gluon jets carrying the total 3-momentum of the parent gluon, not on the details of how gluons fragment to hadrons. The 3 jet momenta or the relative angles between jets then parametrize a "jet Dalitz plot", and these distributions are predicted by the theory.

In sect. 3 we take up phenomenology. We speculate on how a gluon fragments to hadrons, and we discuss distributions in Υ (9.4) decay. We also remark on the 2-jet background process $Q\bar{Q} \to 1\gamma \to q\bar{q} \to 2$ jets, and also on the chances for finding gleuballs *via* (3). Sect. 4 is a summary.

2. Distributions

We assume non-relativistic quarkonium, and we calculate gluon and γ distributions in (1), ignoring internal motion. We also use the Born approximation for $Q\bar{Q} \to 3g$, $Q\bar{Q} \to \gamma + 2g$ (fig. 1). The ignored corrections due to internal motion are $O(v^2/c^2)$, and QCD radiative corrections are $O(\alpha_S/\pi)$(These corrections alter 3g distributions at the α_S/π level, and also lead to events with >3 jets.)

* cf. S. Brodsky et al. [5].

** The search for gluon jets [3] was suggested originally *via* $e^+e^- \to gq\bar{q}$, a QCD radiative correction to $e^+e^- \to q\bar{q}$.

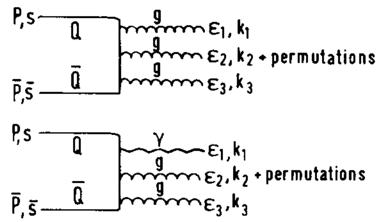

Fig. 1. Feynman diagrams for $Q\bar{Q} \to 3g$, $Q\bar{Q} \to \gamma 2g$, ϵ_i, k_i are gluon (photon) polarizations and momenta.

The $C = -1$ 3g state is symmetric under interchange of color labels and we find the $Q\bar{Q} \to g_i g_j g_k$ matrix element ($i, j, k = 1, \ldots, 8$ are color labels)

$$\mathcal{M}_{ijk} = g_S^3 \tfrac{1}{4}\sqrt{\tfrac{1}{3}}\, d_{ijk}\bar{u}(P, s) \left[\not{\epsilon}_1 \frac{1}{\not{P} - \not{k}_1 - M_Q} \right.$$

$$\left. \times\, \not{\epsilon}_2 \frac{1}{\bar{\not{P}} - \not{k}_3 - M_Q} \not{\epsilon}_3 + \text{permutations} \right] v(\bar{P}, \bar{s}) \,, \tag{4}$$

where momenta and spins are as in fig. 1 (for $\gamma g_i g_j$, replace

$$\tfrac{1}{4} g_S^3 d_{ijk} \to \tfrac{1}{2} g_S^2 e \delta_{ij}) \,.$$

The gluons are exactly massless, and the above is just the ortho-positronium $\to 3\gamma$ amplitude [10] apart from obvious changes in scale.

It will be convenient to parametrize the Dalitz plot of the momenta in terms of dimensionless variables $x_m = 2k_m/M_{Q\bar{Q}} = k_m/M_Q$ ($m = 1, 2, 3$), where $x_m = |\boldsymbol{x}_m|$ are the gluon energies and $x_1 + x_2 + x_3 = 2, \boldsymbol{x}_1 + \boldsymbol{x}_2 + \boldsymbol{x}_3 = \boldsymbol{0}$. In order to describe the spatial orientation of the coplanar 3g state we need a coordinate system [11]. This can be done two ways. We choose a lab frame with $\hat{z} \parallel \boldsymbol{P}_{e^-}$ in $e^+e^- \to Q\bar{Q}$; the x axis is normal to the e^+e^- ring plane and y lies in it (see the appendix). In the first choice of system the Euler angles α, β, γ describe the orientation of the normal to the 3g plane, $\hat{\boldsymbol{n}} \parallel \boldsymbol{k}_1 \times \boldsymbol{k}_2$, β is the polar angle of the normal, $\frac{1}{2}\pi - \alpha$ is its azimuthal angle measured from the ring plane, and γ is a rotation angle between the momentum x_1 and the plane containing the beam axis and the normal. (The last choice treats the gluon momenta asymmetrically.) The second choice uses angles ϕ, θ, χ to describe the orientation of one momentum x_1; θ and $\frac{1}{2}\pi - \phi$ are the polar and azimuthal angles of x_1. The angle χ is the rotation angle between $\boldsymbol{x}_2$ and the plane containing x_1 and the beam. This second system will be useful when we set particle 1 to be the photon in (1).

The calculation of the differential decay rate does not need a specific form for the Q, $\bar{Q}$ spin vectors s_μ, $\bar{s}_\mu$. Then our results are valid for arbitrary beam polarization.

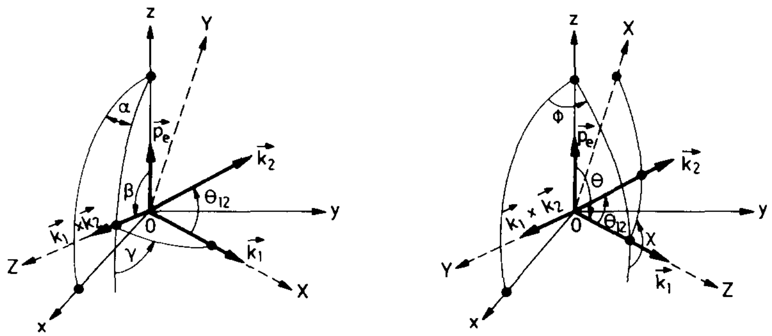

Fig. 2. The two coordinate systems $(\alpha\beta\gamma)$ and $(\phi\theta\chi)$. The former is useful for $Q\bar{Q} \to 3g$ and the latter for $Q\bar{Q} \to \gamma 2g$.

In fact, however, we will only consider natural transverse polarization of e^+e^- here. Then we will need *

$$S_{\mu\nu} = \tfrac{1}{2}(s_\mu \bar{s}_\nu + \bar{s}_\mu s_\nu) = \begin{cases} \tfrac{1}{2}(-1 - P^2) & \mu = \nu = x\,, \\ \\ \tfrac{1}{2}(-1 + P^2) & \mu = \nu = y\,, \end{cases} \tag{5}$$

and $S_{\mu\nu} = 0$ otherwise (P is the e^+ or e^- polarization). We will also need

$$S_{ij} \equiv x_i^\mu S_{\mu\nu} x_j^\nu\ . \tag{6}$$

This in hand, we calculate the differential rate

$$\frac{\mathrm{d}\Gamma}{\mathrm{d}x_1 \mathrm{d}x_2 \mathrm{d}R} = \frac{\sum_{\epsilon_i} |M|^2}{128\pi^3} |\psi_{Q\bar{Q}}(0)|^2$$

$$= \frac{160}{9} \frac{W(x_1, x_2, x_3)}{x_1^2 x_2^2 x_3^2} |\psi_{Q\bar{Q}}(0)|^2\ , \tag{7}$$

$$\Gamma_{3g} = \frac{160}{81}(\pi^2 - 9)\frac{\alpha_S^3}{M_{Q\bar{Q}}^2} |\psi_{Q\bar{Q}}(0)|^2\ ,$$

where $\mathrm{d}R = \mathrm{d}\alpha \mathrm{d}\cos\beta \mathrm{d}\gamma/8\pi^2$ or $\mathrm{d}\phi \mathrm{d}\cos\theta \mathrm{d}\chi/8\pi^2$ and α_S is, of course, the M_Q dependent QCD coupling. In (7) we have

$$W(x_1, x_2, x_3) = x_1^2(1 - x_1)^2 + x_2^2(1 - x_2)^2 + x_3^2(1 - x_3)^2 \tag{8}$$

$$+ \sum_{i \leqslant j = 1}^{3} S_{ij} F_{ij}(x_1, x_2, x_3)\ , \tag{8}$$

* This is easily derived *via* $e^+e^- \to Q\bar{Q} \to \mu^+\mu^-$.

with

$$F_{33}(x_1, x_2, x_3) = \tfrac{1}{2}(x_1^2 + x_2^2) + x_1^2 x_2 + x_1 x_2^2 - \tfrac{3}{2}x_1 x_2 ,$$
$$F_{12}(x_1, x_2, x_3) = x_3 + x_1 x_2(1 - 2x_3) , \tag{8'}$$

and their permutations.

The trace calculation involved was done using REDUCE. The expression for W with $S_{ij} \to 0$ is originally due to Ore and Powell [10]. (8) and (8′) explicitly show the permutation symmetry in $\boldsymbol{k}_1, \boldsymbol{k}_2, \boldsymbol{k}_3$, and allow for arbitrary polarization. We now express this in a more convenient form. In the text we present the formulae for $P^2 = 0$; the case with $P^2 \neq 0$ will be found in the appendix.

The general expression for the angular dependence of $e^+e^- \to 123$ can be written analogously to the case of electroproduction reactions (e.g. $eN \to e\pi N$) *. The angular dependence can be factored out so that the five-fold differential decay rate is $(P^2 = 0)$[11] **

$$\frac{1}{\Gamma_{3g}} \frac{d\Gamma}{dx_1 dx_2 dR} = \frac{27}{8(\pi^2 - 9)} \{\bar{\sigma}_U(1 + \cos^2\beta) + 2\bar{\sigma}_L \sin^2\beta + 2\bar{\sigma}_T \sin^2\beta \cos 2\gamma$$
$$- 2\bar{\sigma}_I \sin^2\beta \sin 2\gamma\} \tag{9}$$

in the first system, and

$$\frac{1}{\Gamma_{3g}} \frac{d\Gamma}{dx_1 dx_2 dR} = \frac{27}{8(\pi^2 - 9)} \{\sigma_U(1 + \cos^2\theta) + 2\sigma_L \sin^2\theta + 2\sigma_T \sin^2\theta \cos 2\chi$$
$$- 4\sqrt{2}\sigma_I \cos\theta \sin\theta \cos\chi\} \tag{10}$$

in the second. (Note that the α or ϕ dependence drops out for $P^2 = 0$.)

The $\bar{\sigma}_a, \sigma_a$; a = U, L, T, I have the following interpretation. $\bar{\sigma}_U(\bar{\sigma}_L)$ are cross sections for virtual photons polarized with spin ±1 (0) along the normal $\hat{\boldsymbol{n}}$; $\bar{\sigma}_T(\bar{\sigma}_I)$ are the real (imaginary) parts of the interference between spin ±1 and ∓1 photons. $\sigma_U(\sigma_L)$ are cross sections for virtual photon spin ±1 (0) along $\boldsymbol{x}_1$; $\sigma_T(\sigma_I)$ are the interference of spin ±1 and ∓1 amplitudes (the real part of spin ±1 and spin-0 interference).

For the $\bar{\sigma}_a$ and σ_a we find in the appendix that

$$\bar{\sigma}_U = \bar{\sigma}_L = \tfrac{2}{3}[x_1^2(1 - x_1)^2 + x_2^2(1 - x_2)^2 + x_3^2(1 - x_3)^2]/x_1^2 x_2^2 x_3^2 ,$$
$$\bar{\sigma}_T = \tfrac{1}{2}\bar{\sigma}_U - \tfrac{1}{3}A \sin^2\theta_{12} ,$$
$$\bar{\sigma}_I = \tfrac{1}{6}[2A \cos\theta_{12} + B] \sin\theta_{12} ; \tag{9'}$$

* We want to thank D. Schiller for unpublished material on $e^+e^- \to 123$ kinematics.
** The normalization is such that integration over R and one of the six identical sectors of the Dalitz plot gives unity.

$$\sigma_U = \tfrac{4}{3}[x_1^2(1-x_1)^2 + x_2^2(1-x_2)^2 + x_3^2(1-x_3)^2]/x_1^2x_2^2x_3^2 - \tfrac{1}{3}A \sin^2\theta_{12} ,$$
$$\sigma_L = \tfrac{1}{3}A \sin^2\theta_{12} ,$$
$$\sigma_T = \tfrac{1}{6}A \sin^2\theta_{12} ,$$
$$\sigma_I = \tfrac{1}{6}\sqrt{\tfrac{1}{2}}[2A\cos\theta_{12} + B]\sin\theta_{12} ; \qquad (10')$$

where

$$A \equiv A(x_1, x_2, x_3) = 2x_2^2[(1-x_3)^2 + (1-x_2)^2]/x_1^2x_2^2x_3^2 ,$$
$$B \equiv B(x_1, x_2, x_3) = 4x_1x_2(1-x_3)^2/x_1^2x_2^2x_3^2 ,$$
$$\cos\theta_{12} = 1 - 2\,\frac{1-x_3}{x_1x_2} ,$$

where θ_{12} is the angle between gluon momenta 1 and 2.

These expressions simplify a lot if we first carry out the integration over γ or χ. In the first case we find the distribution of the normal for a fixed configuration of x_1, x_2, x_3 but without information on the orientation within the 3g plane *

$$\frac{1}{\Gamma_{3g}}\,\frac{d\Gamma}{dx_1dx_2d\cos\beta} = \frac{9}{8(\pi^2-9)}\,[x_1^2(1-x_1)^2 + x_2^2(1-x_2)^2 + x_3^2(1-x_3)^2]$$
$$\times\frac{1}{x_1^2x_2^2x_3^2}\,(2+\sin^2\beta) . \qquad (11)$$

In the second case we find the angular distribution of x_1 (also with fixed x_1, x_2, x_3). Rather than quoting this expression, we prefer to identify $x_1 = x_\gamma = 2E_\gamma/M_{Q\bar{Q}}$ in the process $Q\bar{Q} \to \gamma + 2g$, and then integrate (10′) over x_2, holding x_γ fixed. The result is the inclusive angular distribution of the γ in $e^+e^- \to Q\bar{Q} \to \gamma + 2g \to \gamma +$ hadrons:

$$\frac{1}{\Gamma_{\gamma 2g}}\,\frac{d\Gamma}{dx_\gamma d\cos\theta} = \frac{3}{4(\pi^2-9)}\,[\sigma_0(\chi_\gamma) + \sigma_1(x_\gamma)\cos^2\theta]$$
$$= \frac{3}{4(\pi^2-9)}\,\sigma_0(x_\gamma)[1 + \alpha(x_\gamma)\cos^2\theta] , \qquad (12)$$

for which we find

$$\sigma_0(x) = F(x) + 2G(x) , \qquad \alpha(x) = \frac{\sigma_1(x)}{\sigma_0(x)} ,$$
$$\sigma_1(x) = F(x) - 6G(x) ,$$
$$F(x) = \frac{x(1-x)}{(2-x)^2} + \frac{2-x}{x} + 2\,\frac{(1-x)^2}{(2-x)^3}\ln\frac{1}{1-x} - 2\,\frac{1-x}{x^2}\ln\frac{1}{1-x} , \qquad (12')$$

* The resulting dependence on β is the same as for $e^+e^- \to q\bar{q}g$ [3]; this was first noted by Brodsky et al. [5]. Note that (11) tests the gluon spin; for three $J^P = 0^-(0^+)$ particles in the final state, $\bar{\sigma}_U = 0(\bar{\sigma}_L = 0)$.

$$G(x) = \frac{1-x}{x^4}\left\{\frac{2x(1-x)}{(2-x)^2} - 2x - \frac{4(1-x)}{(2-x)^3}\ln\frac{1}{1-x}\right.$$
$$\left. + 2\frac{4-3x}{(2-x)^2}\ln\frac{1}{1-x} - x\ln\frac{1}{1-x}\right\}. \qquad (12'')$$

In fig. 3 we plot the energy distribution of the γ integrated over θ_γ (it is the same as for unpolarized positronium decay) and the angular distribution function $\alpha(x_\gamma)$ *. QCD predicts both of them. In addition the ratio γgg to ggg is predicted [7],

$$\frac{\Gamma(Q\bar{Q}\to\gamma gg)}{\Gamma(Q\bar{Q}\to ggg)} = \tfrac{36}{5}e_Q^2\frac{\alpha}{\alpha_S}. \qquad (13)$$

We close this section with a discussion of the $\bar{\sigma}_a$, σ_a and some comments on experimental issues. $\bar{\sigma}_U$ and $\bar{\sigma}_L$ are both proportional to the positronium function of Ore and Powell [10]. The only difference in our case is the angular dependence arising from the $Q\bar{Q}$ polarization. The functions $\bar{\sigma}_T$, $\bar{\sigma}_I$ are new. They vanish at the symmetry point $x_1 = x_2 = x_3 = \frac{2}{3}$. This is due to the threefold symmetry of this "star" configuration, and the 2-fold symmetry of the coefficients of $\bar{\sigma}_T$, $\bar{\sigma}_I$. At the boundary, where one of the x_i is unity, $\bar{\sigma}_I$ vanishes and

$$\bar{\sigma}_T\,(\text{boundary}) = \tfrac{1}{2}\bar{\sigma}_{U,L}\,(\text{boundary}).$$

This is due to helicity. At the Dalitz boundary the gluon momenta are collinear. The 3 jets become 2 jets. As gluons are massless, and have $j = 1$, the net spin along this collinear axis is ± 1 and this collinear configuration has an angular distribution forbidden for spinless gluons:

$$\frac{d\Gamma}{d\cos\theta_{jet}} \propto 1 + \cos^2\theta_{jet} \qquad (14)$$

(θ_{jet} is the polar angle of the collinear configuration). This can be verified by direct calculation in either system in the appendix, and it is why $\alpha(x_\gamma) \to 1$ as $x_\gamma \to 1$ in fig. 2. This 2-jet distribution is the *same* as for $e^+e^- \to Q\bar{Q} \to 1\gamma \to q\bar{q} \to 2$ jets. This is important, as it directly tests in a physically transparent way that the vector gluons have no mass and no zero-helicity state.

As a visual aid we show in figs. 4 and 5 Dalitz plots of the σ's and also graphs of the σ's along lines in the Dalitz plot. We remark that $\bar{\sigma}_a$, σ_a are constant along the boundary except for a non-uniform behavior near the corners ($x_i \to 0$)**. As a result, plots which average over a region of x_i will not necessarily show the constant behavior as the corners are approached. Also, there is an asymmetry of e.g. σ_T, σ_I due to our having extracted factors like $\cos x$, $\cos 2x$.

How are these distributions to be measured experimentally? Gluons do not emerge

* $\alpha(x_\gamma) = \alpha(x_{gluon})$ can be used to get the single-hadron angular distribution in $Q\bar{Q} \to 3g \to$ hadron + anything, given a model for gluon $\to$ hadrons.

** This is an artifact of infrared divergences which cancel in the total differential rate.

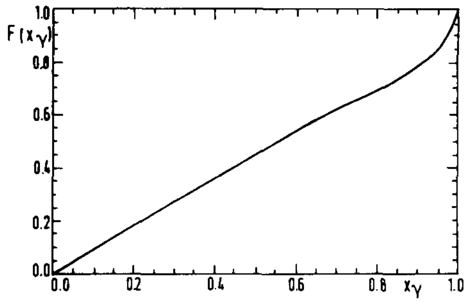

Fig. 3a

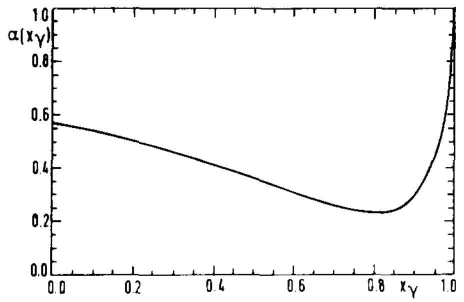

Fig 3b

Fig. 3. (a) Inclusive γ energy distribution for $Q\bar{Q} \to \gamma 2g$, (b) inclusive γ angular distribution function $\alpha(x_\gamma)$ for $Q\bar{Q} \to \gamma 2g$.

in the final state, but we expect jets, each carrying the total 3-momentum of the parent gluon. This does not depend on the details of how gluons fragment to hadrons, but only on the existence of finite-p_T gluon jets *. We imagine that this total jet momentum (or energy plus direction) is measured by a calorimeter. Then asymptotically the scaled jet momenta satisfy $x_{\text{jet}1} = x_1$, $x_{\text{jet}2} = x_2$, $x_{\text{jet}3} = x_3$ and the distributions of these quantities are predicted here. (At finite energies it might be better to plot distributions in relative jet angles $\theta_{12}, \theta_{23}, \theta_{13}$. These also parametrize the Dalitz plot, as $\cos\theta_{ij} = 1 - 2(1 - x_k)/x_i x_j$). Since the total gluon jet 3-momentum does not depend on the number of gluon fragments, all this also works if one makes an experimental cut on final state multiplicities (e.g. $N_{\text{had}} \leqslant 9$ or one can study events of fixed N_{had}).

Even if the inclusive γ in $Q\bar{Q} \to \gamma gg$ cannot be identified on an event-by-event basis, the rate, energy and angular distributions serve as tests of QCD. We expect

* That is, we assume that in a given order in g_S, gluon and quark distributions can be interpreted as jet distributions. The only non-perturbative effects are those given rise to jets having the three momentum of the parent gluon or quark. It may even be possible to produce evidence for gluon jets in QCD (for quark jets, see ref. [12]).

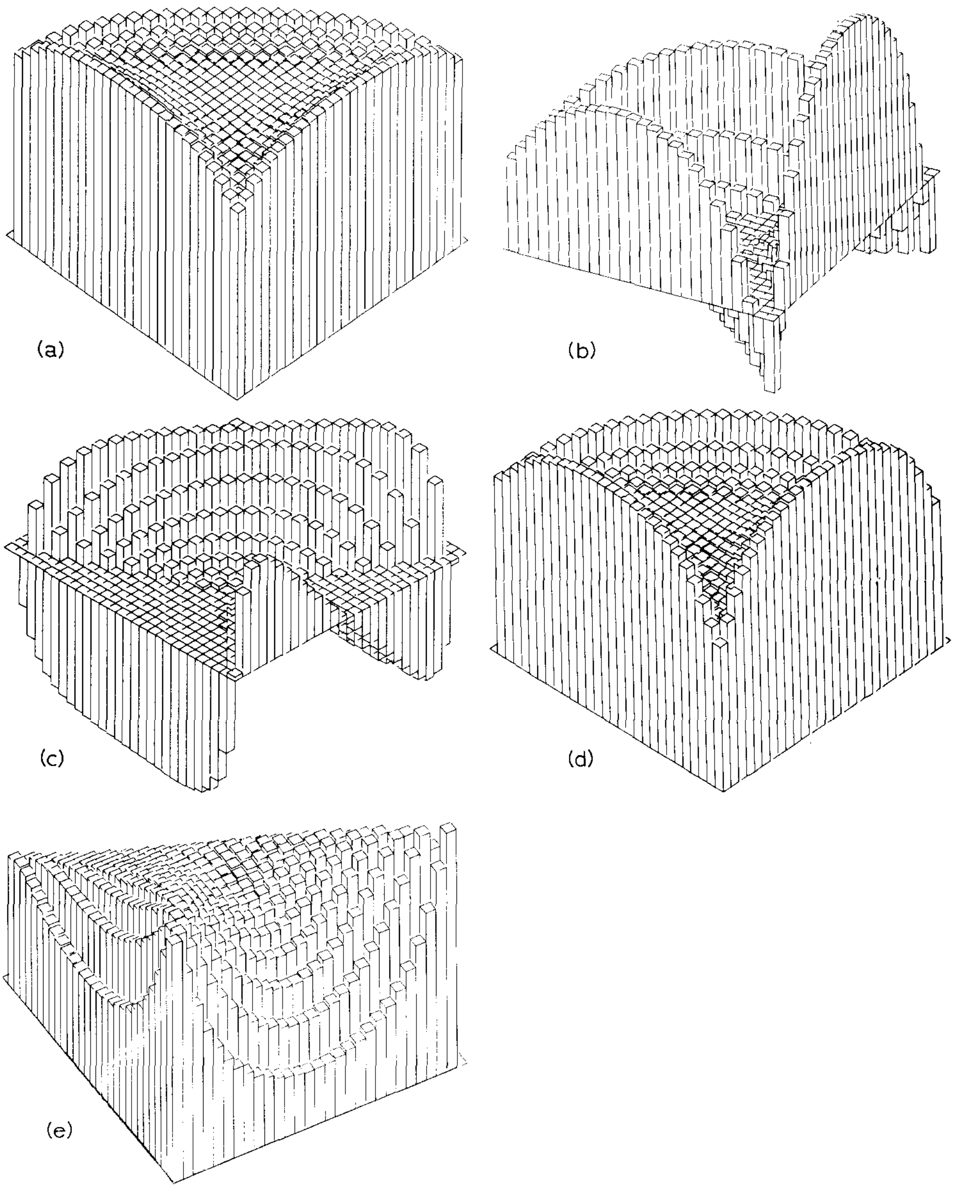

Fig. 4. (a) A view of the 3-gluon Dalitz plot for $\overline{\sigma}_U$. Note that $\overline{\sigma}_U = \overline{\sigma}_L$. (b) A view of the 3g Dalitz plot for $\overline{\sigma}_T$. (c) A view of the 3g Dalitz plot for $\overline{\sigma}_I$. Note that $\overline{\sigma}_I = \sqrt{2}\sigma_I$. (d) A view of the γgg Dalitz plot for σ_U. (e) A view of the γgg Dalitz plot for σ_L. Note that $\sigma_L = 2\sigma_T$.

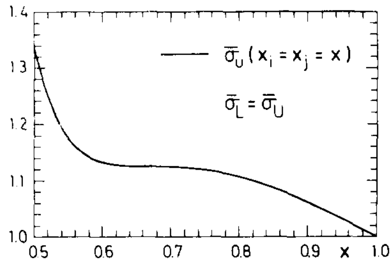

fig. 5a

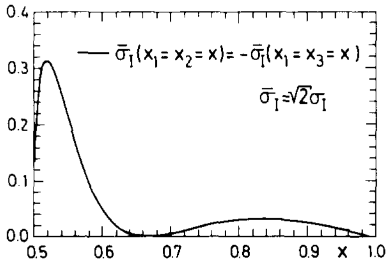

fig. 5b

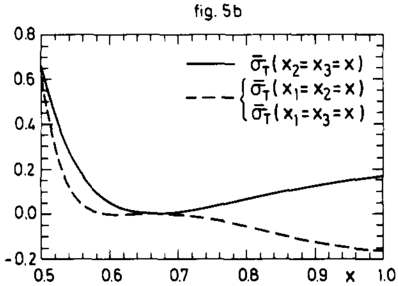

fig. 5c

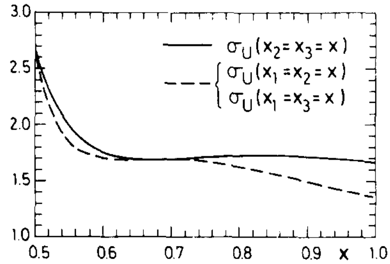

fig. 5d

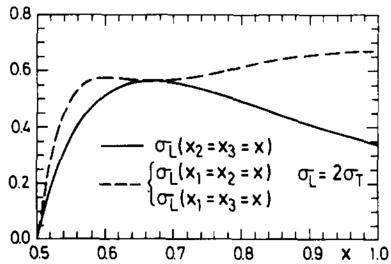

fig. 5e

Fig. 5. (a) Section across the Dalitz plot $\bar{\sigma}_U = \bar{\sigma}_L$ from the middle of one side (left) to the opposite corner (right). There is only one plot because of the symmetry of $\bar{\sigma}_U$. (b) Section across the Dalitz plot $\bar{\sigma}_I$ or $\sqrt{2}\sigma_I$ from one side to the opposite corner for $x_1 = x_2$. Note the sign change ofr $x_2 \rightleftharpoons x_3$. If $x_2 = x_3$, $\bar{\sigma}_I$ is zero. (c) Section across the Dalitz plot for $\bar{\sigma}_T$, as before. Note the symmetry under $x_2 \rightleftharpoons x_3$. (d) Sections across the Dalitz plot for σ_U, as before. (e) Sections across the Dalitz plot for σ_L, as before. Note that $\sigma_L = 2\sigma_T$.

little difficulty with backgrounds from photons from π^0, η decay because of the hard γ spectrum predicted for $Q\bar{Q} \to \gamma gg$.

3. Phenomenology

We concentrate here on hadron distributions and gluon jets at Υ (9.4). Except for $Q\bar{Q} \to \gamma + 2g$, we will not have much to say about J/ψ decay; its mass is too small for our considerations to be useful. (Quark jets are only clean for $P_{\text{quark}} \gtrsim 3$ GeV [2]; we cannot expect the situation to be more favorable for gluon jets.)

The ratios of Υ decays in QCD are

$$
\begin{array}{lllll}
\Upsilon \to e\bar{e} + \mu\bar{\mu} & : \Upsilon \to q\bar{q} + \tau\bar{\tau} & : \Upsilon \to 3g & : \Upsilon \to \gamma 2g & \\
2 & : R & : \dfrac{10(\pi^2 - 9)\,\alpha_S^3}{81\pi\alpha^2 e_Q^2} & : \dfrac{8(\pi^2 - 9)}{9\pi}\dfrac{\alpha_S^2}{\alpha} & \\
2 & : \sim 5 & : \begin{array}{c} 5 \\ 20 \end{array} & : \begin{array}{ll} 1 & e_Q = \frac{2}{3} \\ 1 & e_Q = -\frac{1}{3} \end{array} &
\end{array}
\tag{15}
$$

for $\alpha_s(M_\Upsilon^2) \approx 0.15$ (α_S scales as $(\ln M^2)^{-1}$) [6]. The ratio $\Gamma(Q\bar{Q} \to 3g)/\Gamma_{\text{tot}}$ decreases somewhat at higher M_Q. If $e_Q = -\frac{1}{3}$, $\Gamma(Q\bar{Q} \to 3g)/\Gamma_{\text{tot}} = 0.7$ for Υ and $\sim$0.3 for the next $e_{Q'} = +\frac{2}{3}Q'\bar{Q}'$ state at $\sim$30 GeV *.

In order to judge how hard it will be to find 3g jets at Υ, we need to know how a gluon fragments. QCD is no help, and we must speculate. We adopt the following simple picture. A colored quark can fragment into a string of $q\bar{q}$ pairs ordered uniformly in rapidity from 0 to $y_{\max} = \ln P_{\text{quark}}$. A colored gluon (e.g. with the color index of red and blue quarks) cannot. However, it can fragment into two strings of $q\bar{q}$ pairs, transferring the net color to $y = 0$. We assume that these strings of $q\bar{q}$ are independent. The model is implemented by folding the $g \to q\bar{q}$ distribution of the leading q in each string into the fragmentation function of each q:

$$
D_g^h(z) = \int_z^1 \frac{dx}{x} D_q^h(x)\, D_g^q\!\left(\frac{z}{x}\right) + \int_z^1 \frac{dx}{x} D_{\bar{q}}^h(x)\, D_g^{\bar{q}}\!\left(\frac{z}{x}\right) \tag{16}
$$

(we assume scaling here and in what follows).

Notice that some of the time the gluon can fragment off its mass shell to a high mass $q\bar{q}$ state. This will broaden the gluon jet and occasionally lead to gluon $\to$ 2 jet events ($Q\bar{Q} \to 4$ jets in all). That this plays no role for Υ can be seen by estimating the related probability of a gluon to yield a heavy $c\bar{c}$ state J/ψ [13]:

$$
\frac{\Gamma(\Upsilon \to 3g \to J/\psi + \ldots)}{\Gamma(\Upsilon \to 3g)} \approx \frac{\alpha_s(M_{J/\psi}^2)}{\alpha_s(M_\phi^2)}\,\frac{\Gamma(J/\psi \to 3g \to \phi + \ldots)}{\Gamma(J/\psi \to 3g} \approx \tfrac{1}{2}\% \tag{17}
$$

(the scaled phase space is the same in both). We thus ignore multijet events (or $c\bar{c}$ production *via* $Q\bar{Q} \to 3g \to c\bar{c} + \ldots$) at the Υ. At a very high mass $Q\bar{Q}$ such processes can be $O(\alpha_S/\pi)$ of the 3-jet rate.

For practical estimates we ignore the gluons' polarization and set $D_g^q = \text{const.}$**.

* The mass comes from $M_\phi : M_{J/\psi} : M_\Upsilon : M_? \sim 1 : 3 : 3^2 : 3^3$.

** Summing over ± 1 helicities of g would give $D_g^q(z) \propto z^2 + (1 - z)^2$ as in QED [14].

Then

$$D^{\mathrm{h}}_{\Upsilon}(z) = \int_z^1 \frac{\mathrm{d}x}{x}\, D^{\mathrm{h}}_{\mathrm{g}}(x)\, D^{\mathrm{g}}_{\Upsilon}\left(\frac{z}{x}\right) . \tag{18}$$

Independent of further details, this model implies that multiplicities in Υ decay are large (we estimate [5] $\langle N^{3\mathrm{g}}_{\mathrm{ch}} \rangle \approx 10$, compared to 5 off resonance). This is due to the fact that asymptotically if a quark fragments into $\langle n^{\mathrm{g}}_{\mathrm{ch}} \rangle \sim a \ln P_{\mathrm{q}}$ charged particles, a gluon fragments to $\sim 2a \ln \frac{1}{2} P_{\mathrm{g}}$. The momentum needed to see g jets is also large, about twice the energy needed to see q jets. This indicates that it may be hard to see gluon jets in individual events at Υ *. (A mass $\gtrsim$ 20 GeV would be better.)

We can use (16), (18) to get $D^{\mathrm{h}}_{\Upsilon}$ from $D^{\mathrm{h}}_{\mathrm{q}}$. However, we want to emphasize that (16) can be explioted to extract $D^{\mathrm{h}}_{\mathrm{g}}$ directly. This is simplest when we use the linear approximation $D^{\mathrm{g}}_{\Upsilon}(y) = 6y$, since then

$$D^{\mathrm{h}}_{\mathrm{g}}(z) \propto z^2 \frac{\partial}{\partial z}\left(\frac{1}{z} \frac{\mathrm{d}\tau(\Upsilon \to 3\mathrm{g} \to \mathrm{h} + ...)}{\mathrm{d}z}\right) . \tag{19}$$

In fig. 6 we show $D^{\mathrm{h}}_{\Upsilon}(y)$ using both the linear approximation and the exact $D^{\mathrm{g}}_{\Upsilon}(y)$. In each case we used (16), (18) and (15), $D^{\mathrm{h}}_{\mathrm{q}}(z) = a + b(1 - z)^2$ with $a = 0.05$, $b = 1.05$. Eq. (19) may be useful in extracting $D^{\mathrm{h}}_{\mathrm{g}}$ for use in other reactions involving gluon jets.

We have discussed inclusive spectra in Υ decay elsewhere [5] (e.g. the preponderance of $I = 0$ fast hadrons like ω, ϕ over e.g. ρ^0), and have nothing to add here except to encourage experimentalists to look particularly for $\Upsilon \to \phi + ...$, and $\mathrm{J}/\psi + ...$

Even if 3-jet structure is hard to see in random events it may be evident in low-multiplicity final states. Of course, one looses events this way. As a guide to the loss in events suffered by fixing N_{had}, we assume purely pionic final states (thus N_π is odd for $\Upsilon \to 3\mathrm{g}$, and we ignore N_π even) and use a Poisson distribution for N with $\langle N_\pi \rangle = 15$. In order to ensure $P_{\mathrm{had}} \geqslant 1$ GeV we need $N_{\mathrm{had}} \leqslant 9$. This is 9% of the total $\Upsilon \to 3\mathrm{g} \to N_\pi = \mathrm{odd}$.

Besides the $\Upsilon \to 3\mathrm{g} \to 3$ jet events, it will be interesting to look for the angular distribution of $\Upsilon \to 3\mathrm{g} \to 2$ jet events (collinear 3g events). Once $\Gamma(\Upsilon \to \mathrm{e}^+\mathrm{e}^-)$ is known, so is $\Gamma(\Upsilon \to \mathrm{q}\bar{\mathrm{q}} \to 2$ jets), from data off resonance. Then one can try to study $\Upsilon \to 3\mathrm{g} \to 2$ jet distributions **.

If it is difficult to see 3 jets we can still imagine looking at $\Upsilon \to \gamma\mathrm{gg}$ with E_γ not too large ($E_\gamma \sim 1 - 2$ GeV, say), so as to get a large gluon energy ***.

The decay $\Upsilon \to \gamma\mathrm{gg} \to \gamma$ + hadrons is interesting from another point of view. It

* A good tool for a 3-jet search would be a calorimeter measuring the energy in $\gtrsim 12\pi$ solid angle segments; we estimate that $\gtrsim 0(5\%)$ of $\Upsilon \to 3\mathrm{g} \to$ hadrons will show 3 clear jets in such a calorimeter.

** One might think that $\mathrm{Q}\bar{\mathrm{Q}} \to 1\gamma \to \mathrm{q}\bar{\mathrm{q}}$ jets and $\mathrm{Q}\bar{\mathrm{Q}} \to 3\mathrm{g} \to 2$ jets intefere. This is not so, as quark jets carry flavor and gluon jets do not.

*** $\Upsilon' \to {}^3\mathrm{P}_{0,2}(\mathrm{Q}\bar{\mathrm{Q}}) + \gamma$, ${}^3\mathrm{P}_{0,2} \to \mathrm{gg}$ also delivers 2g jets [16], though it may be difficult to isolate such events.

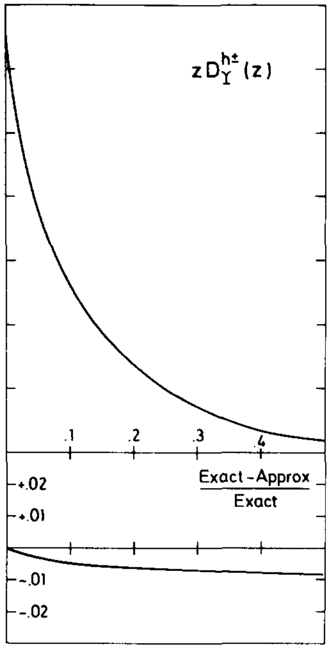

Fig. 6. Distribution function $zD_X^h(z)$ for hadrons from Υ, together with the deviation between the exact expression and our approximation (see text). The deviation is <1% for $z \leqslant 0.8$. Nonscaling effects at small z are ignored.

combines a calculable short-distance contribution $\Upsilon \to \gamma gg$ and an unknown long-distance non-perturbative piece. Namely, this decay allows us access to the color singlet process

$$g + g \to \text{hadrons}$$

as a function of the invariant 2g mass from 0 to M_Υ. (At high invariant mass we of course expect gluon jets). At low invariant mass, the hadron spectrum consists of $q\bar{q}$ resonances. We expect these to have small glue content, and for $M \gtrsim 1$ GeV the Zweig rule [8] tells us that $gg \to q\bar{q}$ is strongly suppressed, typically by a factor $Z^{1/2} \sim 10^{-1}$, where Z is of order $\sigma(\pi N \to \phi N)/\sigma(\pi N \to \omega N) \sim 10^{-2}$(for $C = -$, but we expect the same for $C = +$).

As an application of this observation, if we examine rates for $J/\psi \to \gamma\eta, \gamma\eta'$, $\gamma f(1250)$ (which have been seen [15]), we expect them to fall short of the inclusive QCD process $J/\psi \to \gamma gg$ by $O(Z^{1/2}) \sim 10^{-1}$. We can check this inclusively as follows. We form the integral ($x = M_X^2/M_{J/\psi}^2$ in $J/\psi \to \gamma + M_X$)

$$\Gamma_{x_{max}} = \int_0^{x_{max}} dx \frac{d\Gamma}{dx}, \quad \Gamma_{x_{max}=1} = \Gamma(J/\psi \to \gamma + ...) ,$$

$$M_X^2 = M_{J/\psi}^2(1 - x_\gamma) , \quad x_\gamma = 2E_\gamma/M_{J/\psi} . \tag{20}$$

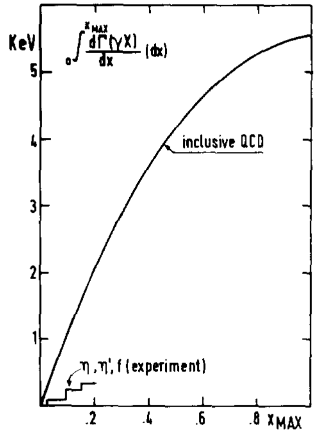

Fig. 7. The integrated radiative decay rate as a function of scaled missing mass $x = M_X^2/M_{J/\psi}^2$ in the reaction $J/\psi \to \gamma + X$. The curve is the QCD prediction and the steps involve measured rates.

In fig. 7 we show $\Gamma_{x_{max}}(J/\psi \to \gamma + \text{hadrons})$ from the inclusive QCD prediction with $\alpha_S = 0.2$ and including recent measurements of $J/\psi \to \gamma\eta, \gamma\eta', \gamma f(1250)$ [17]. The narrow resonances appear as steps in fig. 7. If $gg \to q\bar{q}$ saturated unitarity we would expect these steps to lie around the QCD curve. In fact, they are a factor ~5 lower. (Increasing α_S would increase the QCD curve, and the effect would be more dramatic). The "discrepancy" is near what one would expect from the Zweig rule for $f^0(1250)$; for η, η' it shows that neither has a significant glue component in its wavefunction. We expect that at larger M_X^2, the probability for gg to evolve to hadrons will increase to 100%. But how? This is what can be found out *via* $J/\psi \to \gamma$ + hadrons and $\Upsilon \to \gamma$ + hadrons. In our view, a graph of

$$R_{2g} = \frac{(d\Gamma(Q\bar{Q} \to \gamma + \text{had})/dM_X)_{\text{expt}}}{(d\Gamma(Q\bar{Q} \to \gamma + 2g)/dM_{2g})_{\text{QCD}}} \tag{21}$$

gives the probability directly. (See fig. 8 for some fantasy; note that $C = +, I = 0$ glueballs cannot be too light, or they would already have been seen in $J/\psi \to \gamma\pi^+\pi^-$ or γK^+K^- *via* their two-body decays [17].) * Just as one example, let us suppose that hadronic states of gluons (glueballs [4]) really exist. Then we expect gg → glueballs to average the QCD expectation (unlike $gg \to q\bar{q}$, which does not). Thus we estimate from "gluonic duality" **

$$\text{BR}(J/\psi \to \gamma + \text{glueball}) \approx (5 - 10) \times \text{BR}(J/\psi \to \gamma + q\bar{q}\ \text{state}) \approx 1\% . \tag{22}$$

* It will be interesting to study the M_X and $M_{Q\bar{Q}}$ dependence of (21) using J/ψ, Υ (e.g. ref. [18]; the discrepancy in fig. 7 has been found independently by M. Krammer).

** We assume that glueball and $q\bar{q}$ states are roughly equally spaced in M_X. If the glueball spectrum were denser than $q\bar{q}$ one might see many narrow γ lines near the glueball threshold.

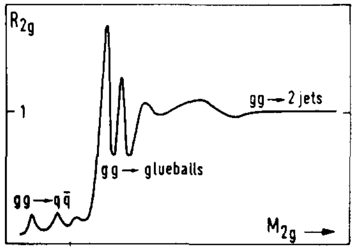

Fig. 8. Fanciful plot of R_{2g}, showing the regions where gg → $q\bar{q}$, gg → gluonic resonances, and gg → gluon jets.

Evidently, J/ψ and $\Upsilon \to \gamma$ + hadrons will be a good way to find glueballs if they exist at all. They will be seen as spikes or bumps in the missing mass recoiling against the γ in $Q\bar{Q} \to \gamma$ + hadrons.

4. Conclusions

In our view, quarkonium decays are an ideal place to verify or refute the basic ideas of QCD. We can look for gluon jets, bound states of gluons, and can check the Born approximation in the perturbation expansion in QCD in the running coupling $g_S = (4\pi\alpha_S)^{1/2}$. Some kinematic features in quarkonium decay will produce evidence that gluons are really massless vector particles.

By contrast, quarkonium decays in Born approximation can offer no *direct* evidence for the non-Abelian character of the theory (self-couplings of the gluons) *. This evidence must be gained in other and probably more painful fashion.

We wish to thank R. Devenish, M. Krammer (particularly for discussions on J/ψ radiative decays), H. Krasemann, H. Salecker and P. Zerwas.

Appendix

In this appendix we present more details on the derivation of the differential cross sections $\bar{\sigma}_a$, σ_a, a = U, L, T, I for the processes $Q\bar{Q} \to 3g$, γgg. For details on the kinematic structure of $e^+e^- \to 3$ particles, we refer the reader to ref. [11].

As stated in the text, we use two coordinate systems $(\alpha\beta\gamma)$ and $(\phi\theta\chi)$ as in fig. 2. The gluon momenta in the $(\alpha\beta\gamma)$ system (used to parametrize $Q\bar{Q} \to 3g$) are given in

* Bound states of gluons would of course be indirect evidence for gluon self-couplings.

terms of the Euler angles by their x, y, z components,

$$k_{1x} = k_1 [\cos\alpha \cos\beta \cos\gamma - \sin\alpha \sin\gamma] ,$$

$$k_{1y} = k_1 [\sin\alpha \cos\beta \cos\gamma + \cos\alpha \sin\gamma] ,$$

$$k_{1z} = -k_1 \sin\beta \cos\gamma ,$$

$$k_{2x} = k_2 [\cos\theta_{12}(\cos\alpha \cos\beta \cos\gamma - \sin\alpha \sin\gamma) - \sin\theta_{12}(\cos\alpha \cos\beta \sin\gamma + \sin\alpha \cos\gamma)] ,$$

$$k_{2y} = k_2 [\cos\theta_{12}(\sin\alpha \cos\beta \cos\gamma + \cos\alpha \sin\gamma) - \sin\theta_{12}(\sin\alpha \cos\beta \sin\gamma - \cos\alpha \cos\gamma)] ,$$

$$k_{2z} = k_2 [-\cos\theta_{12} \sin\beta \cos\gamma + \sin\theta_{12} \sin\beta \sin\gamma] , \qquad \text{(A.1)}$$

where we set $\boldsymbol{k}_3 = -\boldsymbol{k}_1 - \boldsymbol{k}_2$ here and in the following. In the $(\phi\theta\chi)$ system (which we use for $Q\overline{Q} \to \gamma gg$ by identifying k_1 with k_γ in the text) the components are

$$k_{1x} = k_1 \sin\theta \cos\phi ,$$

$$k_{1y} = k_1 \sin\theta \sin\phi ,$$

$$k_{1z} = k_1 \cos\theta ,$$

$$k_{2x} = k_2 [\sin\theta_{12}(\cos\phi \cos\theta \cos\chi - \sin\phi \sin\chi) + \cos\theta_{12} \cos\phi \sin\theta] ,$$

$$k_{2y} = k_2 [\sin\theta_{12}(\sin\phi \cos\theta \cos\chi + \cos\phi \sin\chi) + \cos\theta_{12} \sin\phi \sin\theta] ,$$

$$k_{2z} = k_2 [-\sin\theta_{12} \sin\theta \cos\chi + \cos\theta_{12} \cos\theta] , \qquad \text{(A.2)}$$

with the abbreviations

$$X(\alpha) = -P^2 \cos 2\alpha ,$$

$$Y(\alpha) = +P^2 \sin 2\alpha . \qquad \text{(A.3)}$$

The cross section for $e^+e^- \to 3$ particles with transversely polarized e^+e^- beams take the following form for the $(\alpha\beta\gamma)$ system (3g case):

$$\frac{1}{\Gamma_{3g}} \frac{d\Gamma}{dx_1 dx_2 dR} = \frac{27}{8(\pi^2 - 9)} \{\bar{\sigma}_U(1 + \cos^2\beta + X(\alpha)\sin^2\beta) + 2(1 - X(\alpha))\,\bar{\sigma}_L \sin^2\beta + 2[(\sin^2\beta + X(\alpha)(1 + \cos^2\beta))\cos 2\gamma + 2Y(\alpha)\cos\beta \sin 2\gamma]\,\bar{\sigma}_T - 2[(\sin^2\beta + X(\alpha)(1 + \cos^2\beta))\sin 2\gamma - 2Y(\alpha)\cos\beta\cos 2\gamma]\,\bar{\sigma}_I\} , \qquad \text{(A.4)}$$

and in the $(\phi\theta\chi)$ system (γgg case) *

$$\frac{1}{\Gamma_{3g}}\frac{d\Gamma}{dx_1dx_2dR}=\frac{27}{8(\pi^2-9)}\{(1+\cos^2\theta+X(\phi)\sin^2\theta)\,\sigma_U$$
$$+2(1-X(\phi))\sin^2\theta\sigma_L$$
$$+2[(\sin^2\theta+X(\phi)(1+\cos^2\theta))\cos 2\chi+2Y(\phi)\cos\theta\sin 2\chi]\,\sigma_T$$
$$-4\sqrt{2}[(1-X(\phi))\cos\theta\cos\chi-Y(\phi)\sin\chi]\sin\theta\sigma_I\}\ . \tag{A.5}$$

In these expressions we have abbreviated

$$\frac{d\bar{\Gamma}_a}{dx_1dx_2}\equiv\bar{\sigma}_a\ ,\quad \frac{d\Gamma_a}{dx_1dx_2}=\sigma_a\ ,\quad a=\mathrm{U,L,T,I}\ ,$$

and have chosen the conventional signs for the polarization. The general form (A.4), (A.5) can be obtained from ref. [11]. In the event of longitudinal e^+e^- beam polarization there will be a fifth σ. The σ's are related to spin structure functions by [11]

$$\bar{\sigma}_U=c(R^{11}+R^{-1-1})\ ,\qquad \bar{\sigma}_L=cR^{00}\ ,$$
$$\bar{\sigma}_T=c\mathrm{Re}R^{-1-1}\ ,\qquad \bar{\sigma}_I=c\mathrm{Im}R^{1-1}\ ; \tag{A.6}$$
$$\sigma_U=c(T^{11}+T^{-1-1})\ ,\qquad \sigma_L=cT^{00}\ ,$$
$$\sigma_T=cT^{1-1}\ ,\qquad \sigma_I=\mathrm{Re}T^{10}\ ; \tag{A.7}$$

where c is a coefficient of proportionality and in the first system the superscripts refer to virtual photon (or $Q\bar{Q}$) polarization along the 3g normal; in the second system they are spin projections along $\boldsymbol{k}_1$.

The T's and R's are related to one another by [11]

$$R^{11}=\tfrac{1}{2}(T^{11}+T^{00}-T^{1-1}+2\sqrt{2}\ \mathrm{Im}\,T^{10})\ ,$$
$$R^{1-1}=\tfrac{1}{2}(T^{11}+T^{00}-T^{1-1}-2\sqrt{2}\ \mathrm{Im}\,T^{10})\ ,$$
$$R^{00}=T^{11}+T^{1-1}\ ,$$
$$R^{1-1}=\tfrac{1}{2}(T^{11}-T^{00}-T^{1-1}+i2\sqrt{2}\ \mathrm{Re}\,T^{10})\ , \tag{A.8}$$

which we use to get the following identities among the σ's:

$$\bar{\sigma}_U=\tfrac{1}{2}\sigma_U+\sigma_L-\sigma_T\ ,$$
$$\bar{\sigma}_L=\tfrac{1}{2}\sigma_U+\sigma_T\ ,$$
$$\bar{\sigma}_T=\tfrac{1}{2}(\tfrac{1}{2}\sigma_U-\sigma_L-\sigma_T)\ ,$$
$$\bar{\sigma}_I=\sqrt{2}\sigma_I\ , \tag{A.9}$$

on taking $T^{11}=T^{-1-1}$ into account (it follows from parity).

* We write this for 3g; for γgg there is a different statistics factor.

We have verified the general structure (A.4), (A.5) and have derived the σ's explicitly in both the $(\alpha\beta\gamma)$ and $(\phi\theta\chi)$ systems. In this appendix we merely determine the $\overline{\sigma}$'s; the σ's then follow from the relations (A.8).

In order to determine $\overline{\sigma}_a$ it is sufficient to put $P^2 = 0$ in (A.4) and integrate over either γ (to project out $\overline{\sigma}_U, \overline{\sigma}_L$) or over β (to project out $\overline{\sigma}_T, \overline{\sigma}_I$) and compare the results with corresponding formulas obtained from (7), (8). To do this we need the explicit Euler angle dependence of

$$S_{ij} \equiv x_i^\mu S_{\mu\nu} x_j^\nu = -\tfrac{1}{2}[x_{ix}x_{jx} + x_{iy} + P^2(x_{ix}x_{jx} - x_{iy}x_{jy})] , \qquad \text{(A.10)}$$

where the components of $\boldsymbol{x}_i$ are given by (A.1) and $\boldsymbol{x}_i = 2\boldsymbol{k}i/M_{Q\overline{Q}}$. The α integration is trivial, and integrating over γ we obtain from (A.4) with $P^2 = 0$ on the one hand

$$\frac{1}{\Gamma_{3g}} \frac{d\Gamma}{dx_1 dx_2 d\cos\beta} = \frac{27}{16(\pi^2 - 9)} [(1 + \cos^2\beta)\overline{\sigma}_U + 2\sin^2\beta\overline{\sigma}_L] , \qquad \text{(A.11)}$$

and from (7), (8) on the other hand

$$\frac{1}{\Gamma_{3g}} \frac{d\Gamma}{dx_1 dx_2 d\cos\beta} = \frac{9}{8(\pi^2 - 9)} H(x_1, x_2, x_3)(2 + \sin^2\beta) , \qquad \text{(A.12)}$$

where $H = H(x_1, x_2, x_3)$ is the Ore-Powell function

$$H = [x_1^2(1 - x_1)^2 + x_2^2(1 - x_2)^2 + x_3^2(1 - x_3)^2]/x_1^2 x_2^2 x_3^2 . \qquad \text{(A.13)}$$

Thus

$$\overline{\sigma}_U = \overline{\sigma}_L = \tfrac{2}{3}H . \qquad \text{(A.14)}$$

In order to obtain $\overline{\sigma}_T$ and $\overline{\sigma}_I$ we integrate over β, finding

$$\frac{1}{\Gamma_{3g}} \frac{d\Gamma}{dx_1 dx_2 d\gamma/2\pi} = \frac{9}{\pi^2 - 9} \{\tfrac{2}{3}H + \tfrac{1}{2}(\cos 2\gamma\overline{\sigma}_T - \sin 2\gamma\overline{\sigma}_I)\} . \qquad \text{(A.15)}$$

We compare this with the β-integrated expression of (7),

$$\frac{1}{\Gamma_{3g}} \frac{d\Gamma}{dx_1 dx_2 d\gamma/2\pi} = \frac{9}{\pi^2 - 9} \left\{\tfrac{2}{3}H + \frac{C}{12}[\cos 2\gamma\cos\theta_{12} - \sin 2\gamma\sin\theta_{12}] + \tfrac{1}{12}(A' - A)\cos 2\gamma\right\} , \qquad \text{(A.16)}$$

where C, A, A' are functions of the original F_{ij}'s in (8′):

$$C \equiv C(x_1, x_2, x_3) = 2A\cos\theta_{12} + B , \qquad \text{(A.17)}$$

$$A \equiv A(x_1, x_2, x_3) = 2x_2^2(F_{33} + F_{22} - F_{23})/x_1^2 x_2^2 x_3^2$$
$$= 2((1 - x_3)^2 + (1 - x_2)^2)/x_1^2 x_3^2 , \qquad \text{(A.18)}$$

$$A' \equiv A'(x_1, x_2, x_3) = 2x_1^2(F_{33} + F_{11} - F_{13})/x_1^2 x_2^2 x_3^2$$
$$= 2((1 - x_3)^2 + (1 - x_1)^2)/x_2^2 x_3^2 , \qquad \text{(A.19)}$$

$$B \equiv B(x_1, x_2, x_3) = 2x_1 x_2(F_{12} + 2F_{33} - F_{13} - F_{23})/x_1^2 x_2^2 x_3^2$$
$$= 4(1 - x_3)^2/x_1 x_2 x_3^2 ; \qquad \text{(A.20)}$$

note that $\cos\theta_{12} = 1 - 2(1 - x_3)/x_1x_2$. Comparison of (A.15) with (A.16) then gives

$$\bar{\sigma}_T = \tfrac{1}{6}C\cos\theta_{12} + \tfrac{1}{6}(A' - A) = \tfrac{1}{3}(H - A\sin^2\theta_{12}) , \qquad \text{(A.21)}$$

$$\bar{\sigma}_I = \tfrac{1}{6}C\sin\theta_{12}$$

We have derived the σ_a, a = U, L, T, I in the same way, but here we simply use (A.9) to obtain directly

$$\sigma_U = \tfrac{3}{2}\bar{\sigma}_U + \bar{\sigma}_T ,$$

$$\sigma_L = \tfrac{1}{2}\bar{\sigma}_U - \bar{\sigma}_T = 2\sigma_T ,$$

$$\sigma_I = \sqrt{\tfrac{1}{2}}\bar{\sigma}_I . \qquad \text{(A.22)}$$

Their explicit forms on the Dalitz triangle can be found in the text, (10′).

References

[1] H. Fritzsch, M. Gell-Mann and H. Leutwyler, Phys. Lett. B47 (1973) 365;
D.J. Gross and F. Wilczek, Phys. Rev. D8 (1973) 3497;
S. Weinberg, Phys. Rev. Lett. 31 (1973) 31.
[2] R. Schwitters, Symp. on Lepton and photon interactions at high energies, Stanford, 1975.
[3] J. Ellis, M.K. Gaillard and G.G. Ross, Nucl. Phys. B111 (1976) 253;
T.A. De Grand, Y.J. Ng and S.-H. Tye, Phys. Rev. D16 3251 (1977);
S. Brodsky, 12th Rencontre de Moriond, March 1977 SLAC-PUB-1937 (May 1977).
[4] D. Robson, Nucl. Phys. B130 (1977) 328, and references therein.
[5] K. Koller and T.F. Walsh, Phys. Lett. 72B (1977) 227 (E: 73B (1978) 504);
T.A. De Grand et al., ref. [3].
S. Brodsky, D.G. Coyne, T.A. De Grand and R.R. Horgan, SLAC-PUB-2047;
H. Fritzsch and K.-H. Streng, CERN preprint TH 2435.
[6] T. Appelquist and H.D. Politzer, Phys. Rev. Lett. 34 (1975) 43, Phys. Rev. D12 (1975) 1404;
H.D. Politzer, Caltech preprint CALT-68-628.
[7] M. Chanowitz, Phys. Rev. D12 (1975) 912;
L. Okun and M. Voloshin, Moscow preprint ITEP-95 (1976).
[8] S. Okubo, Phys. Lett. 5 (1963) 165;
G. Zweig, CERN TH 401, 412 (1964);
Iizuka, Prog. Theor. Phys. Suppl. 37-38 (1968) 21.
[9] O. Nachtmann, Int. Symp. on Lepton and photon interactions at high energies, Hamburg, 1977.
[10] A. Ore and J.L. Powell, Phys. Rev. 75 (1949) 1696.
[11] N.M. Avram and D.H. Schiller, Nucl. Phys. B70 (1974) 272.
[12] G. Sterman and S. Weinberg, Phys. Rev. Lett. 39 (1977) 1436.
[13] F. Vanucci et al., ψ (3095) decays involving ϕ, unpublished.
[14] M. Chen and P. Zerwas, Phys. Rev. D12 (1976) 187.
[15] L. Sehgal, Int. Symp. on Lepton and photon interactions at high energies, Hamburg, 1977.
[16] M. Krammer and H. Krasemann, Phys. Lett. 73B (1978) 58;
A. de Rujula, J. Ellis, E.G. Floratos and M.K. Gaillard, Nucl. Phys. B138 (1978) 387.
[17] W. Bartel et al., Phys. Lett. 64B (1976) 479; 66B (1976) 489;
W. Braunschweig et al., Phys. Lett. 67B (1977) 243;
PLUTO collaboration, DESY preprint 77/72;
DASP collaboration, DESY preprint 78/01.
[18] M. Krammer, DESY preprint 78/06; Rencontre de Moriond. March 1978